

Numerical Method for Generating Orthogonal Curvilinear Meshes¹

W. D. BARFIELD

Los Alamos Scientific Laboratory, Los Alamos, New Mexico 87544

Received May 12, 1969

ABSTRACT

The method is based on conformal mapping of the boundary of a closed two-dimensional region on the perimeter of a rectangular polygon in which is inscribed an orthogonal rectilinear grid. Features of the method and the associated numerical analysis are described. A numerical scheme for interpolating lines between the orthogonal curvilinear mesh lines in order to match lines to specified points on the boundary is presented. Examples of orthogonal meshes inscribed in various geometrical figures are included.

This paper describes a numerical method for inscribing an orthogonal curvilinear mesh (OCM) in a closed, simply connected, nonself-overlapping two-dimensional region \mathcal{R} . Essentially, the method consists of finding the function which conformally maps the boundary of the given region \mathcal{R} (Fig. 1) onto the boundary of a rectangular

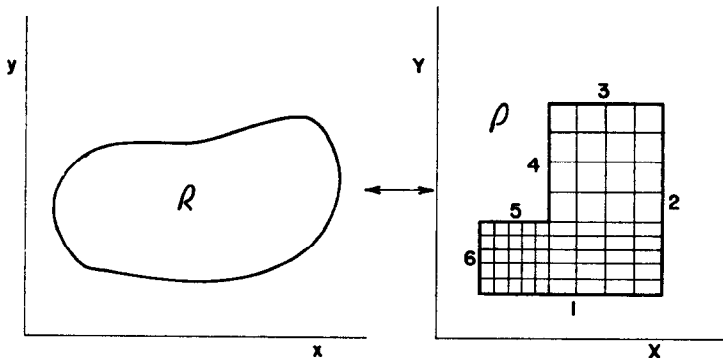


FIG. 1. The boundary of the region \mathcal{R} is mapped conformally onto the boundary of a rectangular polygon \mathcal{P} . The image of an orthogonal rectilinear grid in \mathcal{P} is an orthogonal curvilinear mesh inscribed in \mathcal{R} .

¹ Work performed under the auspices of the U.S. Atomic Energy Commission.

polygon \mathcal{P} (i.e., a polygon all of whose exterior angles are $\pm\pi/2$) and then using the mapping function so determined to find the image of an orthogonal rectilinear grid inscribed in the rectangular polygon. The N arbitrarily selected points of the boundary of \mathcal{R} can be made to correspond to the N corners of the rectangular polygon. An interpolation scheme for fairing curves between the lines of the OCM so generated in order to match lines to selected points along portions of the boundary of the region \mathcal{R} is also described.

The conformal mapping is done in three steps: The region \mathcal{R} is mapped into the unit circle $|w| \leq 1$ by the transformation

$$w(z) = e^{\Gamma(z, z_0)}, \quad (1)$$

where $z = x + iy$, and $\Gamma(z, z_0) =$ complex Green's function [1] for the region \mathcal{R} . The transformation takes the point z_0 into the center of the unit circle. The unit circle is mapped into the rectangular polygon \mathcal{P} by the conformal transformations

$$w(z') = \frac{z' - i}{z' + i}, \quad (2)$$

where z' is real for $|w| = 1$, and

$$X + iY = A \int_0^{z'} \prod_{j=1}^N (\xi - \bar{x}_j)^{\pm 1/2} d\xi \quad (3)$$

(Schwarz-Christoffel transformation). $\bar{x}_j =$ image in real axis ($\text{Im } z' = 0$) of j th corner point.

The complex Green's function for the region \mathcal{R} has the form

$$\Gamma(z, z_0) = \log(z - z_0) + g(z) + ih(z),$$

where the logarithm is the potential of a unit source ("line charge") at an interior point z_0 , and $g + ih$ is an analytic function in \mathcal{R} determined by the requirement that

$$\text{Re } \Gamma(z, z_0) = 0, \quad z \in C,$$

where C is the boundary of \mathcal{R} ; i.e.,

$$g(z) = -\log |z - z_0|, \quad z \in C.$$

Introducing a single-layer source density distribution $\sigma(\zeta)$ on C for the potential $g(z)$, the preceding equation becomes a singular integral equation for the determination of $\sigma(\zeta)$ [2]:

$$-\log |z - z_0| = \int_C \log |z - \zeta| \sigma(\zeta) d\zeta, \quad (z \in C). \quad (4)$$

Adding the imaginary part the nonsingular part of the complex Green's function is obtained:

$$g(z) + ih(z) = \int_C \log(z - \zeta) \sigma(\zeta) |d\zeta|, \quad z \in \mathcal{R}$$

NUMERICAL ANALYSIS

The singular integral equation (4) for the source density σ is solved numerically by the method of Symm [2], in which the integral is replaced by a numerical quadrature (Simpson's $\frac{1}{3}$ - rule) so that the integral equation reduces to an $N_0 \times N_0$ linear system, where N_0 is the number of Simpson integration intervals around the boundary of \mathcal{R} . Once the "corners"² have been chosen, the overall

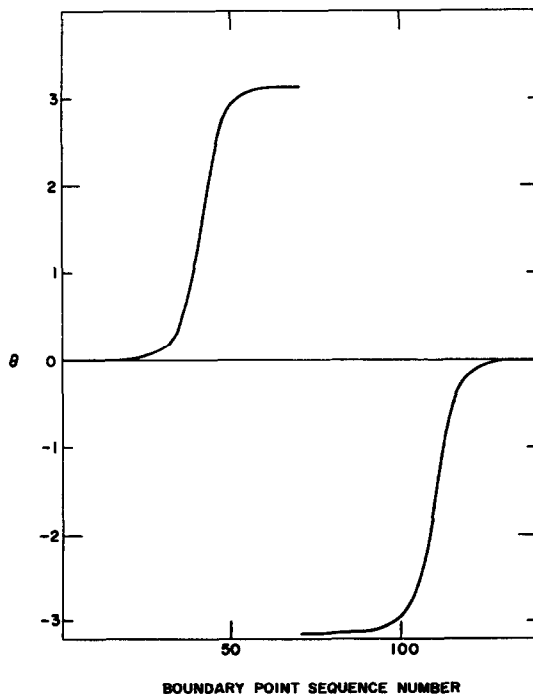


FIG. 2. Map in unit circle of an elongated parallelogram (Fig. 6). The corners of the parallelogram correspond to boundary points numbers 1, 23, 70, 92, where point 1 is the lower left-hand corner.

² A "corner" in \mathcal{R} is the image of a corner of \mathcal{P} ; "side" refers to the (curved) portion of the boundary of \mathcal{R} between two "corners."

mapping is independent of the choice of z_0 . Best results are obtained if the image in \mathcal{R} of the point (1, 0) of the unit circle—corresponding to $x' \rightarrow \infty$ in (3)—is chosen to lie on one of the longer “sides” (in \mathcal{R}) about midway between two “corners.”³ The standard linear system solver in use at Los Alamos, which uses Gauss elimination with nonmaximal pivoting and accumulation of inner products in double precision, [3] was found to give satisfactory results.

The map in the unit circle of the boundary of an *elongated* region \mathcal{R} characteristically shows nearly flat portions corresponding to the portions of the boundary of \mathcal{R} farthest removed from z_0 (e.g., Fig. 2). The effect of numerical error of the mapping thus tends to be magnified for such portions of the boundary, and has the practical effect of limiting the applicability of the method to regions not more than about twice as long as broad. (However, elongated regions can be subdivided into less elongated subregions: See example below.) Because of this effect, the point z_0 should be centrally located in \mathcal{R} .

The values of \bar{x}_j , the images on the real axis ($\text{Im } z' = 0$) of the “corners,” are determined from Eqs. (1) and (2). The $\int_{\bar{x}_i}^{\bar{x}_{i+1}}$ in (3) is approximated by N_1 Simpson intervals.⁴ The ratio of real and imaginary parts of the constant A in (3) is determined so as to bring the sides of the image (in X, Y space) of the boundary of \mathcal{R} parallel to the coordinate axes. Each side of the rotated image is divided into a number of equal intervals ΔX or ΔY . The boundary nodal points so determined are mapped onto the boundary of \mathcal{R} by use of the mapping functions (2) and (3) and linear interpolation in the table of $\arg w$ (central angle in unit circle) vs boundary point sequence number, giving a set of image points $\zeta_i = x_i + iy_i$ on the boundary of \mathcal{R} . The partial S/C integrals $\int_{x_{i-1}}^{x_i'}$ are approximated by Simpson

³ The phases of the logarithms were determined by requiring that

$$-\pi \leq \arg(z_{j+1} - z_{i+1}) - \arg(z_{j+1} - z_i) \leq \pi$$

and

$$-\pi \leq \arg(z_{j+1} - z_{i+2}) - \arg(z_{j+1} - z_i) \leq \pi \quad (i \neq j),$$

and

$$0 \leq \arg(z_{j+1} - z_{j+2}) - \arg(z_{j+1} - z_j) < 2\pi.$$

⁴ The singularity in the integrand of the S/C integral (3) when $x' = \bar{x}_i$ and the corresponding exponent is $-\frac{1}{2}$ is removed by rewriting the integral as [1]

$$\int_0^{\bar{x}_i} (\xi - \bar{x}_i)^{-1/2} \left[\prod_{j \neq i}' (\xi - \bar{x}_j)^{\pm 1/2} - K \right] d\xi - 2iK(\bar{x}_i)^{1/2},$$

where

$$K = \prod_{j \neq i}' (\bar{x}_i - \bar{x}_j)^{\pm 1/2}.$$

The new integrand $\rightarrow 0$ as $\xi \rightarrow \bar{x}_i$.

quadrature with N_2 intervals, where N_2 depends on $DXP = |x'_{i-1} - x'_{i-2}|$ (Table I). The value of x'_i is found by a Newton iteration using the value of x'_{i-1}

TABLE I

	N_2
$DXP \leq 0.1$	2
$0.1 < DXP \leq 0.4$	6
$0.4 < DXP \leq 1.0$	24
$1.0 < DXP \leq 2.0$	50
$2.0 < DXP$	100

as a guess, except when x'_{i-1} is the image of a corner. In the latter case an approximate analytical solution, valid near a corner, is used to obtain a guess for x'_i :

$$XGES = \bar{x}_j + \left\{ \frac{(1 - k_j)(\Delta X + i\Delta Y)}{A \prod'_{m \neq j} (\bar{x}_j - \bar{x}_m)^{-k_m}} \right\}^{1/1-k_j},$$

where $k_j = \pm \frac{1}{2}$ and either ΔX or ΔY is 0.

The images of the interior mesh points are found by numerical solution of Laplace equations⁵

$$x_{XX} + x_{YY} = 0,$$

$$y_{XX} + y_{YY} = 0,$$

with the boundary points $\zeta_i(X_i, Y_i)$ specified, using the simple five-point difference scheme and the point-successive over-relaxation method. In cases where \mathcal{P} has more than four corners, so that there may be more than one value each of $\Delta X, \Delta Y$ (e.g., Fig. 1), the second derivative at a transition line $\Delta X_+ - \Delta X_-$ is approximated by

$$\phi_{XX}(X_1) \approx 2 \frac{\Delta X_- \phi(X_1 + \Delta X_+) - (\Delta X_- + \Delta X_+) \phi(X_1) + \Delta X_+ \phi(X_1 - \Delta X_-)}{\Delta X_- \Delta X_+ (\Delta X_+ + \Delta X_-)} + O(\Delta X),$$

for example. The value of the S.O.R. parameter λ corresponding to a circumscribing rectangle is used, i.e.,

$$\lambda^{1/2} = \frac{1}{2} \left\{ \cos \left(\frac{\pi}{N_X} \right) + \cos \left(\frac{\pi}{N_Y} \right) \right\}.$$

⁵ The images of the interior points could be found by direct evaluation of the mapping functions, of course. For each mesh point this would involve evaluating an integral around the boundary of \mathcal{R} . Note that the Laplace equations are solved on the rectangular polygon \mathcal{P} .

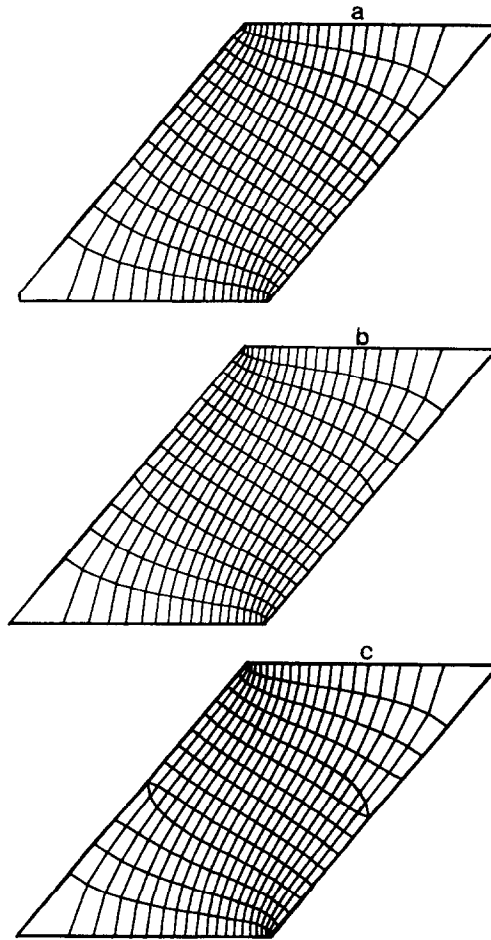


FIG. 3. Effects of various choices of the parameter N_0 = number of Simpson integration intervals around boundary. (a) $N_0 = 138$, (b) $N_0 = 68$, (c) $N_0 = 32$.

Figures 3a–3c show the effect of different choices of N_0 , the number of Simpson integration intervals around the boundary of \mathcal{R} . The different choices $N_1 = 100$, $N_1 = 20$ made a difference of less than 0.15% in the values of the real and imaginary parts of the S/C integral $\int_{x_i}^{x_i+\Delta} f$ for this example.⁶

⁶ It can be shown that for a general region with curved boundary the truncation error in Symm's method for approximating the Fredholm equation (4) is $O(|\Delta z|)$. A more accurate method— $O(|\Delta z|^2)$ —has been developed by Dr. J. K. Hayes (unpublished AEC report LA-4004, 1968). When σ 's computed by Hayes' method are used in Symm's quadrature for the h function, a smooth monotonic map is obtained for an elongated (1×11) rectangle.

MATCHING LINES

If OCM are separately inscribed in contiguous subregions, the mesh lines will generally not match along the common boundary (e.g., Fig. 8). However, lines can be interpolated⁷ between the lines of the original OCM in order to match lines along certain sides, i.e., to lines in adjacent subregions. Lines cannot be matched along opposite sides of a subregion. (In the *L*-shaped subregion of Fig. 1, for example, lines could be matched along sides 3, 4, 5, and 6, but not along sides 1 and 2. The “*L*” could be subdivided into two rectangles, of course, enabling matching along sides 1 and 2 instead of 3, 4, 5, 6). Figure 4 illustrates how a large

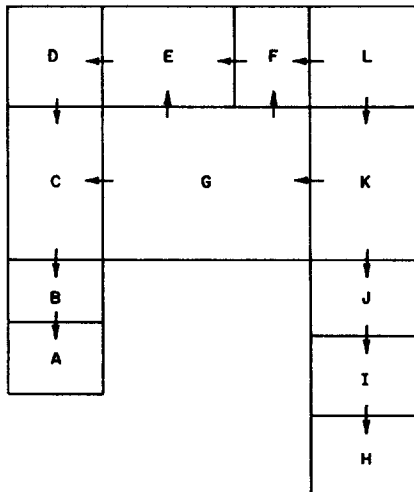


FIG. 4. Illustrates how a large region consisting of several subregions might be zoned with OCM: The region is imagined to be zoned by inscribing an OCM in Subregion A, continuing with B, C, and so on, matching lines as indicated by the directions of the arrows.

region consisting of several subregions might be zoned with OCM: The region is imagined to be zoned by inscribing an OCM in Subregion A, continuing with B, C, and so on, matching lines as indicated by the directions of the arrows. In some cases it may be necessary to subdivide in order to match corners of the logical mesh on opposite sides of a subregion.

It was found that a combination of first-order interpolation for the boundary points and third-order for the interior points gave satisfactory results (e.g., Figs.

⁷ Clearly, any transformation of the form $X' = X'(X)$, $Y' = Y'(Y)$ which preserves orthogonality of the rectilinear mesh in \mathcal{P} gives rise to another OCM in \mathcal{R} .

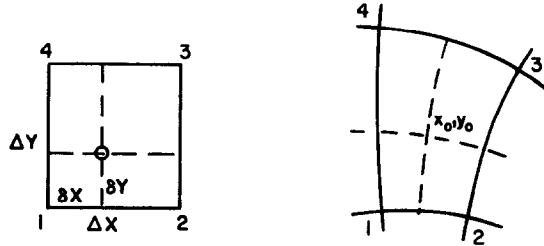


FIG. 5. Interpolation in a single mesh unit. Points 1-4 belong to the original OCM.

7-10).⁸ The third-order interpolation equations at an interior point (x_0, y_0) (Fig. 5) are derived by expanding the coordinates of the four surrounding points of the original OCM and making use of the Cauchy-Riemann relations. The first interpolation equation is

$$x_1 = x_0 - \delta X x_{X0} - \delta Y x_{Y0} + \frac{1}{2}[(\delta X)^2 - (\delta Y)^2] x_{XX0} - \delta X \delta Y x_{XY0} \\ - \frac{1}{2}[\frac{1}{3}(\delta X)^3 - \delta X(\delta Y)^2] x_{XXX0} - \frac{1}{2}[-(\delta X)^2 \delta Y + \frac{1}{3}(\delta Y)^3] y_{XX0}.$$

The δX and δY are determined by first-order interpolation along the subregion boundary. The system of eight third-order equations is solved for the coordinates of the interpolated interior point (x_0, y_0) by eliminating the unknown partial derivatives.

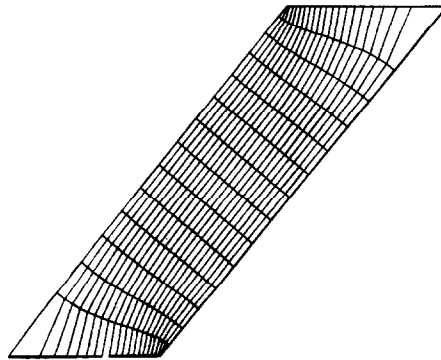


FIG. 6. (Described in text.)

⁸ Better results might be obtained if third-order interpolation were used for the boundary points as well. This would necessitate solving a system of 8 nonlinear algebraic equations to find the interpolation parameters at each boundary point.

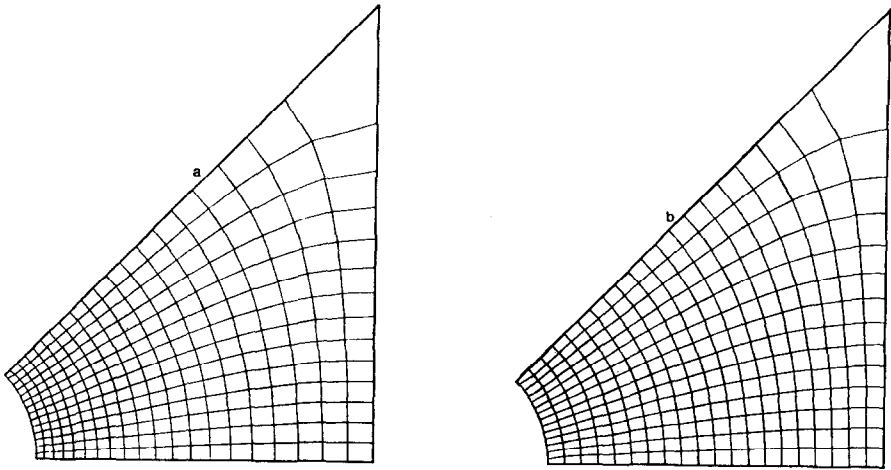


FIG. 7. (Described in text.)

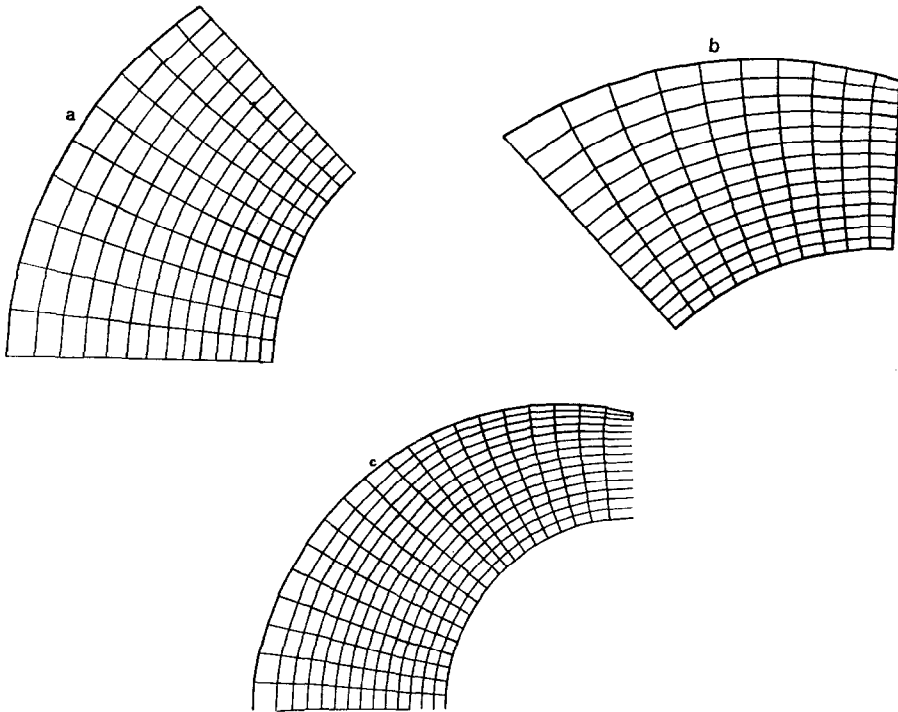


FIG. 8. (Described in text.)

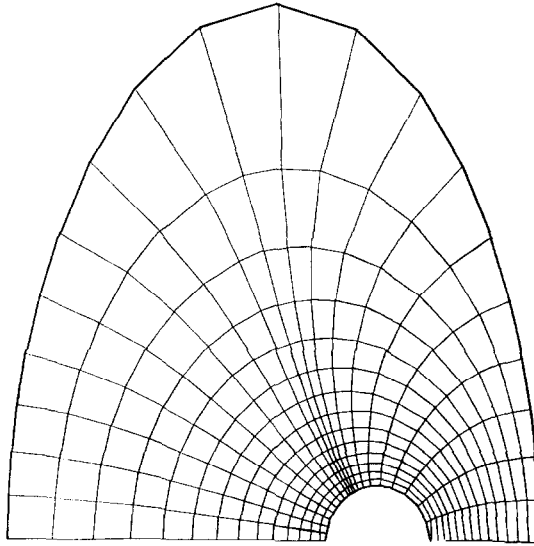


FIG. 9. (Described in text.)

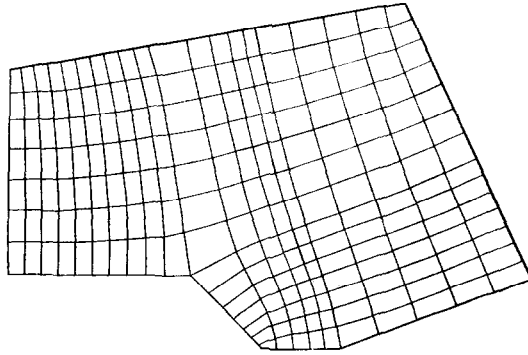


FIG. 10. (Described in text.)

EXAMPLES

Figures 6–10 are an assortment of examples of application of the method.⁹ In Fig. 7(b) the matching feature was used to make the lines equispaced along the bottom edge. The elongated region bounded by two circular arcs and rays (Fig. 8(c)) was subdivided into two parts along a ray; the lines were matched along

⁹ The figures were generated by an automatic plotter which approximates the curved mesh lines by straight-line segments.

the common boundary. In Fig. 9 lines were matched to the intersections with the ellipse of rays making equal angles at the center of the ellipse. In Fig. 10 an OCM corresponding to an L -shaped polygon \mathcal{P} is inscribed in a figure with seven corners. The matching feature was used to space the lines so that a line goes to the odd corner.

A typical example (Fig. 7(a)) required about 16 sec of central-processor time on the CDC-6600 computer, of which ~ 10 sec was spent finding the complex Green's function for the region \mathcal{R} (includes ~ 4 sec solving a 137×137 linear system) and ~ 2 sec was spent solving Laplace's equations (50 iterations) for the interior mesh points. A time of 1.5 sec was required for the interpolation of Fig. 7(b).

CURVILINEAR COORDINATES

The method described here was developed as a zoner/rezoner for Lagrangean hydrodynamic calculations in two space dimensions. However, it is anticipated that application of the method will not be limited to that type of problem. In some applications it will be convenient to regard the families of curves $X = \text{const.}$, $Y = \text{const.}$ as orthogonal curvilinear *coordinates*.¹⁰ The components of the metric of the corresponding coordinate transformation are

$$g_{11} = \left(\frac{\partial x}{\partial X}\right)^2 + \left(\frac{\partial y}{\partial X}\right)^2, \quad g_{22} = \left(\frac{\partial x}{\partial Y}\right)^2 + \left(\frac{\partial y}{\partial Y}\right)^2,$$

$$g_{12} = g_{21} = 0,$$

where (x, y) are the Cartesian coordinates. The first-order partial derivatives at a point (x, y) are conveniently obtained correct to second order in $\Delta X, \Delta Y$ by solution of a set of equations similar to the third-order interpolation equations.

ACKNOWLEDGMENT

The author is indebted to Dr. Blair Swartz for calling his attention to Ref. 2. The automatic mesh-plotting routine was made available by Dr. Thomas Godfrey.

REFERENCES

1. C. GRAM (Ed.), "Selected Numerical Methods . . .," pp.154-173. Regnecentralen, Copenhagen, 1962.
2. G. T. SYMM, *Num. Math.* **9**, 250-58 (1966).
3. PAUL HARPER AND B. L. BUZBEE (private communication).
4. J. L. ANDERSON, S. PREISER, AND E. L. RUBIN, *J. Comp. Phys.* **2**, 279 (1968).

¹⁰ The Eulerian hydrodynamic equations have been given in conservation form for general curvilinear coordinates by Anderson, *et al.*